Passive and Active Airborne Microwave Remote Sensing of Snow Cover*

J. Sokol[1], T.J. Pultz[2], A.E. Walker[3]

[1] Noetix Research Inc.
265 Carling Ave., Suite 403, Ottawa, Ontario, Canada K1S 2E1
[2] Canada Centre for Remote Sensing
588 Booth Street, Ottawa, Ontario, Canada K1A 0Y7
[3] Atmospheric Environment Service
4905 Dufferin Street, Downsview, Ontario, Canada M3H 5T4

ABSTRACT

The presence of snow cover affects the regional energy and water balance, thus having a significant impact on the global climate system. Temporal knowledge of the onset of snow melt and snow water equivalent values are important variables in the prediction of flooding and water resource applications such as reservoir management and agricultural activities. Microwave remote sensing techniques have been demonstrated to be effective for monitoring snow pack parameters (areal extent, depth, water equivalent, wet/dry state). Microwave sensors have all weather imaging capabilities and are sensitive to changes in the dielectric constant within a snow pack.

Coincident airborne polarimetric C-band SAR and microwave radiometer data at 19, 37, and 85 GHz were collected on December 1, 1997, March 6, 1998, and March 12, 1998, over the study are in Eastern Ontario, Canada. Field measurements of snow pack properties and weather conditions were gathered along flight lines on bare agriculture fields during each airborne data acquisition. The multi-temporal, multi-sensor data were analyzed with respect to changes in the SAR polarimetric signatures and microwave brightness temperatures as a function of changing snow pack parameters. This paper will present the results of the investigation comparing SAR and passive microwave values of derived snow parameters. This research initiative is a collaborative investigation between Atmospheric Environment Service (AES) and the Canada Centre for Remote Sensing (CCRS).

INTRODUCTION

Snow parameters are extremely important for input to hydrological models and for understanding changes in the climate system due to global warming. Remote sensing of snow parameters such as snow extent, snow water equivalent, and wet/dry state have been investigated by numerous researchers using various sensors, some to a greater degree of success than others (Goodison et al., 1984; Shi, 1994; Pultz and Crevier, 1996; Bernier and Fortin, 1998). Ground-based observation stations are often very sparse and unevenly spatially distributed, labour intensive, time consuming, and expensive compared to the regional coverage provided by remote sensing techniques. Microwave remote sensing techniques have an advantage over optical methods in that they have all-weather imaging capabilities, and are independent of sunlight, thus increasing image acquisition opportunities. Changes and complexities in the snow pack structure will alter the scattering mechanisms and allow for estimates of snow parameters to be made. Two types of microwave remote sensing techniques were utilized in this research study: passive microwave radiometry and polarimetric Synthetic Aperture Radar (SAR).

Passive microwave energy emitted from the underlying ground surface is transmitted through the snow layer into the atmosphere and recorded by the sensor. Snow pack structure affects the amount of energy received at the sensor, thereby permitting estimates of snow water equivalent (SWE) from brightness temperature values. Ice layers and complex snow packs (multi-layered) obstruct the passive microwave energy, thus reducing brightness temperature values and resulting in overestimates of SWE. Wet snow within a snow pack reduces the volume scattering component and results in a near-blackbody emission (Matzler and Huppi, 1989). SWE estimates decrease when

* Presented at the Fourth International Airborne Remote Sensing Conference and Exhibition/21st Canadian Symposium on Remote Sensing, Ottawa Canada, 21-24 June 1999.

liquid water is present, as absorption of microwave radiation occurs. Brightness temperatures from wet snow conditions and snow-free conditions are very close, thus making it difficult to distinguish between these two states. The two SWE algorithms used in this research were empirically derived from airborne microwave radiometer data sets acquired over agricultural land in the Canadian Prairies (Goodison, et al., 1984). The first algorithm, SWE1, is the dual frequency algorithm using the temperature gradient between the 37 GHz and 19GHZ vertical polarization. The second algorithm, SWE2, is a single frequency algorithm, incorporating the 37 GHz vertical polarization.

Active radar (SAR) sensors are highly sensitive to changes in the dielectric constant and have a better spatial resolution than their passive counterparts. The relationship between snow pack characteristics and radar backscatter are quite complex. Many inconsistencies exist in the literature regarding deriving SWE and snow parameters from airborne and satellite SAR imagery (Bernier and Fortin, 1998; Leconte and Pultz, 1990). SAR backscatter is influenced by a number of parameters including surface roughness, topography, land cover, and moisture content. Multipolarized or polarization diversity SAR systems transmit microwave energy in either a horizontal (H) or vertical (V) orientations towards the target of interest. The orientation of the scattered wave received at the sensor (either horizontal (H) or vertical (V)) is a function of the geometric characteristics and physical properties of the ground target. Polarimetric SARs not only record the 4 mutually coherent polarizations (HH, VV, HV, VH), but also retain phase information during data processing. As a result, these systems provide information on the complete scattering matrix of targets and permit the synthesis of all possible transmit-receive polarizations. By retaining the phase information, a number of other parameters can be generated to characterize the interaction of electromagnetic waves with the targets of interest.

One of the main obstacles in both passive microwave and polarimetric SAR remote sensing of snow cover is the complexities of the snow structure itself. As the snow pack ages, metamorphism occurs resulting in the once homogenous snow structure developing layers of various grain sizes, densities, bonding and textures. With passive microwave sensors, the energy is emitted from the soil layer and travels towards the air/snow interface; the entire snow pack structure is relevant and must be accounted for. With radar remote sensing techniques, microwave energy is transmitted towards the snow surface. This energy can penetrate into the snow structure, can be absorbed or scattered from the snow and/or ground surface, or a combination of these processes can occur. This paper discusses changes in airborne multi-temporal radar backscatter and microwave brightness temperatures as a function of snow pack parameters recorded during the winter of 1997/98.

STUDY AREA LOCATION

The study region is located approximately 50 km east of Ottawa, Ontario (Canada), in an area dominated by agricultural land use. The principal study line runs in an east-west direction just north-west of the town of Casselman, Ontario. This region is located in the seasonal snow cover zone, typically experiencing snowfall between the months of November through to April. According to the 1961-90 climate normal, the average snow depth for the Ottawa International Airport for the end of January is 30 cm (Environment Canada, 1993). The region often experiences a melt event during mid-winter, in January/February, when maximum temperatures increase above zero for a short period of time. During the 1997/98 winter season a complex snow structure developed due to the fluctuation of temperatures and the multiple freezing rain events that occurred in early January.

Sampling points were located on open agricultural fields. Under these conditions, a wind crust generally develops on the top portion of the snow pack and snow redistribution occurs, increasing the variability of snow depth throughout the fields. Sampling takes place along both sides of the county road, approximately 30 meters in from the road, reducing the effect of roads and ditches on snow conditions. The placement of the study sites parallel to the flight line stabilizes the effect of incidence angle. Land cover, soil type, latitude and longitude coordinates (from a Global Positioning System (GPS)) were established for each site.

DATA DESCRIPTION

At this present time, 3 images from the airborne active and passive sensors have been investigated. The airborne

passive microwave sensor consists of three dual-polarization microwave radiometers operating at 19, 37, and 85 GHz frequencies flown on-board a Twin Otter aircraft (Table 1). The active microwave measurements are recorded by a C-band polarimetric radar system on-board a Convair 580. Passive and active airborne acquisitions occurred within 3-4 hours of each other between morning to early afternoon.

Table 1 Data Specifications

	Passive Microwave (Twin Otter)	Polarimetric Radar (Convair 580)
Frequency (GHz)	19, 37, 85 (H&V)	5.3
Flying Altitude (meters)	440	6,100
Incidence Angles	53°	60° - 64°
Spatial Resolution	130m, 80m	Range 6m, Azimuth 1m

A homogenous area within each study site on December 1, 1997, March 6,1998 and March 12, 1998 images were selected and processed using software developed at CCRS and provided by Touzi. C-band linear polarizations, co-polarization plots and polarimetric parameters were generated for each study site. The list of parameters analyzed in this investigation are: sigma nought parameters ($\sigma°_{HH}$, $\sigma°_{VV}$, $\sigma°_{HV}$) pedestal height, total power, co-polarized ratio, and cross-polarized ratio.

Linear co-polarized microwaves ($\sigma°_{HH}$, $\sigma°_{VV}$) are more sensitive than $\sigma°_{HV}$ to the orientation of the target relative to the transmitted polarization. Depolarization of incident waves, as recorded with HV, can also provide information on the scattering mechanisms within the target. Pedestal height is a response to significant volume and multiple scattering (Van Zyl *et al*.,1987). Total power is the sum of the 4 linear polarization's (HH, VV, HV,VH) and is related to the roughness of the target relative to the radar wavelength (Small and Cumming, 1991). The co-polarized ratio (HH/VV) and cross-polarized ratio (HV/ HH) measure the strength of the difference between the linear polarizations. As the co-polarized ratio values approach one, there is insignificant or random structure in the target. The cross-polarized ratio is an indication of the depolarization of horizontal and vertical waves**.** Phase varies with time and distance, therefore the co-polarized phase difference is the difference between the horizontal and vertical phase which can be related to target physical properties. Table 2 through Table 4 contains the polarimetric SAR parameters for December 1, 1997, March 6, 1998 and March 12, 1998, respectively.

Table 2 March 6, 1998 (Wet Snow)

Site	Pedestal Height	Co-polarized Ratio (VV/HH)	Cross-pol Ratio (HV/HH)	σHH (dB)	σVV (dB)	σHV (dB)	Total Power (dB)	Incidence Angle (°)	Sample Size (# pixels)
A	0.31	1.18	0.17	-21.05	-20.87	-29.31	-17.35	61.89	19316
B	0.24	1.05	0.16	-21.12	-21.46	-28.83	-17.57	61.85	24125
E	0.27	1.03	0.14	-22.49	-22.83	-31.05	-19.06	61.76	22657
F	0.31	0.96	0.17	-20.88	-21.55	-28.72	-17.48	61.82	19392
G	0.16	0.96	0.18	-19.92	-20.52	-27.66	-16.48	60.76	17157
H	0.34	0.92	0.08	-17.51	-18.18	-30.43	-14.59	60.81	3906
I	0.25	0.94	0.13	-21.37	-21.85	-29.91	-17.99	60.91	19800
J	0.26	0.82	0.12	-20.81	-21.97	-28.80	-17.62	60.88	13572
Mean	0.27	0.98	0.15	-20.64	-21.15	-29.34	-17.27	61.34	
STDEV (s)	0.06	0.11	0.03	1.45	1.39	1.08	1.30	0.53	

Table 3 March 12, 1998 (Dry Snow)

Site	Pedestal Height	Co-polarized Ratio (VV/HH)	Cross-pol Ratio (HV/HH)	σ HH (dB)	σ VV (dB)	σ HV (dB)	Total Power (dB)	Incidence Angle (°)	Sample Size (# pixels)
A	0.53	1.50	0.16	-13.17	-12.46	-22.16	-9.31	63.22	19116
B	0.52	1.58	0.16	-13.63	-12.80	-22.65	-9.72	62.67	12592
E	0.56	1.37	0.17	-14.84	-14.43	-23.29	-11.07	62.25	15312
F	0.59	1.28	0.18	-14.15	-13.92	-22.26	-10.41	62.38	15488
G	0.60	1.28	0.14	-13.17	-13.13	-22.51	-9.66	61.21	12440
H	0.51	1.38	0.08	-13.33	-12.81	-25.25	-9.80	61.21	22950
I	0.58	1.19	0.16	-15.03	-15.44	-23.50	-11.61	61.41	13640
J	0.58	1.13	0.15	-14.74	-15.10	-23.76	-11.37	61.52	9258
Mean	0.56	1.34	0.15	-14.01	-13.76	-23.17	-10.37	61.98	
STDEV (s)	0.03	0.15	0.03	0.78	1.13	1.02	0.88	0.75	

Table 4 December 1, 1997

Site	Pedestal Height	Co-polarized Ratio (VV/HH)	Cross-pol Ratio (HV/HH)	σ HH (dB)	σ VV (dB)	σ HV (dB)	Total Power (dB)	Incidence Angle (°)	Sample Size (# pixels)
A	0.44	1.39	0.23	-13.02	-12.37	-20.34	-8.99	62.44	16353
B	0.40	1.53	0.29	-15.62	-14.38	-21.70	-11.12	62.07	11242
E	0.43	1.61	0.09	-15.50	-14.10	-21.36	-10.88	61.72	15239
F	0.43	1.69	0.34	-16.45	-16.28	-21.91	-11.67	61.70	19855
G	0.38	1.39	0.16	-13.91	-13.22	-22.55	-10.02	60.99	17429
H	0.30	1.46	0.24	-13.83	-12.88	-20.78	-9.60	60.89	25874
I	0.40	1.63	0.25	-17.51	-16.11	-24.42	-13.06	60.50	12209
J	0.45	1.59	0.33	-15.84	-14.54	-21.49	-11.23	60.64	8220
Mean	0.40	1.54	0.24	-15.21	-14.24	-21.82	-10.82	61.37	
STDEV (s)	0.05	0.11	0.08	1.50	1.42	1.25	1.28	0.71	

Measurements were taken on target fields, using the Surface Roughness Measurement System (SRM-200) on November 20, 1997 and April 6, 1998, prior to snow data collection and after snow melt (Johnson et al., 1993). The SRM is an optical device designed to measure the surface roughness of small areas using a photogrammetric system (Johnson et al., 1993). A selected few fields were measured in both November and April to assess the changes in surface roughness that occurred over the winter season. The surface roughness measurements are represented as the standard deviation of the surface height variation (RMS)(mm). The values for each of the study sites are categorized as smooth or rough according to the Fraunhofer criterion (Ulaby, 1986). All the fields under investigation were classified as rough under C-band wavelengths, thus allowing comparisons between all the fields sampled.

At each sampling location along the flight line snow pack measurements, site photos, and weather conditions were taken. A total of 15 random snow depth measurements were taken in a circle around the sampling location. For SWE values, either the Eastern Snow Conference (ESC-30) tube or the Federal Snow Tube were used to collect the measurements. The diameter of the snow tubes differ slightly, however the resulting measurements are similar and therefore the SWE values are used interchangeably. On the December 1st and March 6th data acquisitions, 2 SWE samples were taken at each site. Difficulties were encountered taking SWE measures on March 12th due to the

complex re-frozen snow pack on March 12th. Therefore, individual measurements of snow and ice layers were taken, and estimated SWE measurements derived. Mean values of ground data are presented in Table 5.

Table 5 Mean Values Recorded During Ground Data Acquisitions

Acquisition Date	Snow State	Mean SWE (mm)	Mean Air Temp (°C)	Mean Snow Depth (cm)	Ground Frozen	Ice Layers
December 1, 1997	DRY	28	-4	17	top 2cm	NO
March 6, 1998	WET	103	0.9	25	YES	YES
March 12, 1998	DRY	63-90*	-13	22	YES	YES

Detailed snow pit and stratigraphy measurements were made on all sampling dates. Figure 1 illustrates snow pack structure for all three sampling dates. An open pit of approximately 1 meter squared was carefully prepared with a clear vertical face on one side of the pit to make the measurements. Snow depth, snow structure, grain sizes, ice layers and temperature of snow layers were recorded. The dielectric constant of the snow surface and mid-pack were measured with a snow capacitance probe.

This analysis will focus on the airborne acquisitions and ground data collection which took place on December 1, 1997, March 6 and 12, 1998. Snow pack conditions were extremely different on each of these dates. The season's snow pack began developing around mid-November when a substantial amount of snow was received on November 14, 1997. Minimum temperatures remained below zero from mid-November until the first acquisition on December 1st, although maximum temperatures fluctuated around zero. A snowfall of 11cm fell on November 30th, the day before the first acquisition, with both maximum and minimum temperatures below zero on both days.

A severe ice storm affected the region in January and deposited up to 4 cm of freezing rain on the snow pack over a period of 24 hours. A stratified snow pack with a solid ice layer between two snow layers resulted. During the week prior to March 6th, maximum temperatures were consistently above zero, resulting in the onset of snowmelt. Minimum temperatures remained below zero during this time period causing snow grains to melt and join together during the day and refreeze at night although significant depletion of the snow pack did not occur. Ground data were collected during mid-day when temperatures exceeded zero, therefore ground measurements taken were representative of wet snow conditions. Just prior to the March 12th acquisition, on the evening of the March 10th, maximum and minimum temperatures dropped well below zero causing the snow pack to solidly refreeze. As a result of numerous melt/refreeze cycles during the previous week, the ice layer had began to melt into the underlying snow layer which then developed into multi-complex layers of ice and snow/ice grains. The entire snow pack was solid, refrozen snow/ice grains, except for a few centimeters of new, dry snow recently fallen on top of the snow pack. Snow pack conditions observed on all three sampling dates were significantly different, and the scattering properties associated with the two snow types also differed and will be discussed in the results.

Passive microwave SSM/I brightness temperature data and SWE values derived from the two AES algorithms for all image dates were acquired by AES. Both SWE1 and SWE2 algorithm values were analyzed and the differences between results discussed (Figure 2).

RESULTS

Preliminary analysis of the co-polarization plots and multi-polarized radar backscatter parameters reflect differences in snow conditions between the acquisition dates. Linear polarization values (σ°_{HH}, σ°_{HV}, σ°_{VV}) between all dates did exhibit differences. Mean linear polarization values for December 1st and March 12th are within 1.5 dB of each other, whereas the March 6th values were up to 8 dB lower due to wet snow conditions. On each image date, σ°_{HH} and σ°_{VV} values were similar, indicating relatively little horizontal or vertical structure in the target. The linear cross-polarization values are significantly lower than HH and VV values for each date. The linear polarization values for all dates resemble scattering responses for wet and dry snow, as reported in the literature (Ulably and Dobson, 1989).

Pedestal height values for all three dates differed significantly. The average pedestal height value for December 1st was 0.4, March 6th was 0.27 and 0.56 for March 12th. The low pedestal height value for March 6th is a result of the wet snow. Due to the high moisture content of the snow surface, minimal volume scattering was likely occurring. Scattering was suspected to occur in only the top portion of the snow structure due to dramatic changes in the dielectric constant. The 0.4 value for December 1st is due to the large volume of new snow and granular snow at the base of the snow pack. The higher pedestal height values for March 12th are related to the greater penetration into the dry snow pack, and therefore increased volume scattering due to the complex snow structure.

The co-polarized ratio values for March 6th approached one, indicating no dominant vertical or horizontal structure in the target, due to the snow surface scattering component. However, mean values for December 1st and March 12th are higher, indicating the radar penetrated further into the dry snow pack. The cross-polarized ratio values are similar for March 6th and 12th and higher on December 1st. The co-polarized phase difference values approached zero on all acquisition dates, therefore HH & VV are in phase. December 1st and March 12th total power values were very similar, although March 6th values appear 6 dB lower. Total power differences between these dates reflects the fact that all linear polarizations for March 6th are much lower. The co-polarization plots for December 1st and March 12th look relatively similar, however σ°_{HH} and σ°_{VV} values are closer in value for March 12th. The plots generated for March 6th have similar linear polarizations values (Ellipticity Angle equal to zero), although σ°_{VV} values are slightly higher. Polarization plots will be presented at the conference.

The output values of the AES SWE algorithms were generally comparable to the ground SWE measurements on all sampling dates (Figure 3). SWE1 and SWE2 values follow the same general trends over the flight line on all dates. SWE2 generally estimates slightly higher than SWE1. On December 1st and March 6th, SWE values are similar, with SWE2 slightly higher than SWE1. On March 12th, SWE2 values are significantly higher by approximately 150mm. SWE1 values decreased on March 12th due to the 19 GHz brightness temperatures dropping significantly relative to the 37GHz brightness temperatures (although values still higher than 37 GHz). The SWE2 values, which are derived from 37V, are overestimated due to changes in snow pack structure. SWE algorithm values slightly underestimate ground SWE on December 1st. This is typically what happens at the beginning of the season when the ground is not completely frozen, and a light snow pack with little structure exists. The dramatic decreases in SWE estimates are a result of frozen streams crossing the flight line path.

DISCUSSION

Changes in weather conditions and snow state between acquisition dates resulted in several SAR parameters showing significant differences, while others indicated no difference. Linear polarizations differentiated between wet and dry snow cover with values differing up to 8 dB on March 6th. The pedestal height parameter also exhibited significant changes between dates, indicating a decrease in volume scattering on March 6th (wet snow date), and increasing values with increasing snow structure. Changes in wet and dry snow conditions were not detected by the passive microwave data due to differences in acquisition times for each data set. However, SWE algorithm values did exhibit differences between dates due to differences in snow structure and temperature. For December 1st and March 6th SWE values approximated ground measurements relatively well, and on March 12th a complex snow structure resulted in a large difference between the two algorithms.

This research has indicated that polarimetric radar parameters are sensitive to snow pack conditions. A number of SAR parameters (linear polarizations, pedestal height, co-polarized ratio, co-polarimetric plots) exhibited significant differences between wet and dry snow conditions, and pedestal height reacted to volume scattering indicating snow structure. While other parameters, such as the co-polarized phase difference values, remained unchanged between the image dates. SAR polarimetric parameters provide information on snow state (wet/dry) and structure within the snow pack; conditions which complicate the extraction of SWE measurements from passive microwave data.

Both passive and active remote sensing techniques of snow cover have strengths and weaknesses. Active techniques can clearly indicate and map the areal extent of wet snow, whereas under the same conditions passive brightness temperature values are similar to “no snow” values. Under dry snow conditions, passive techniques produce SWE estimates. However, complex snow structures, which polarimetric SAR parameters can identify, affect the accuracy

of SWE estimates. By using the strengths of these two techniques, snow state can be monitored under many conditions more accurately than with only one technique. Further research in the field of integrating of passive and active microwave remote sensing techniques to monitor snow cover will provide a more comprehensive analysis of existing snow state and changing conditions.

REFERENCES

Bernier, M., J-P. Fortin. 1998. The Potential of Time Series of C-Band SAR Data to Monitor Dry and Shallow Snow Cover. *IEEE Transactions on Geoscience and Remote Sensing, Vol.36, No. 1, pp. 226-243.*

Environment Canada. 1993. Canadian Climate Normals 1961-90. Canadian Climate Program, pp. 128.

Goodison, B.E, A. Banga, and R.A. Halliday. 1984. Canada-United States Prairie Snow Cover Runoff Study. *Canadian Water Resources Journal, Vol. 9, No. 1, pp. 99-107*.

Johnson, F., B. Brisco and R.J. Brown. 1993. "Evaluation of Limits to the Performance of the Surface Roughness Meter", *Can. J. Remote Sens.*, 19:140-145.

Leconte,R. T.J. Pultz. 1990. Utilization of SAR Data in the Monitoring of Snowpack, Wetlands and River Ice Conditions. *Workshop on Applications of Remote Sensing in Hydrology, Saskatoon, Saskatchewan, February 13-14, pp. 233-247*.

Matzler, C. and R. Huppi. 1989. Review of Signatures studies for Microwave Remote Sensing of Snow Packs. *Advanced Space Research, Vol. 9, No. 1, pp. 253-265.*

Pultz, T.J. and Y. Crevier. 1996. Early Demonstrations of RADARSAT for Applications in Hydrology. *Proceeding of the Third International Workshop, NHRI Symposium, No. 17, October 1996, Greenbelt, Maryland, USA.*

Shi, Jiancheng. 1994. Active Microwave Remote Sensing of Snow Cover. In *Proceeding of the Second International Workshop, NHRI Symposium, No. 14, October 1994, Saskatoon, Saskatchewan.*

Small, D. and I. Cumming. 1991. Evaluation Study on Multi-Frequency Polarimetric SAR, Final Report, pp. 102.

Ulaby, F.T. and M.C. Dobson. 1989. Handbook of Radar Scattering Statistics for Terrain. Artech House LTD, Norwood, MA.

Ulaby, F.T., R.K. Moore, and A.K. Fung. 1986. Microwave Remote Sensing: Active and Passive, Volume II Radar Remote Sensing and Surface Scattering and Emission Theory. *Artech House.*

Van Zyl, J.J., H.A. Zebker, C. Elachi. 1987. Imaging Radar Polarization Signatures: Theory and Observation. *Radio Science, Vol. 22, pp. 529-543*.

ACKNOWLEGEMENTS

Special thanks to Heather McNairn of the Canada Centre for Remote Sensing for reviewing this paper, to Stefan Nedelcu of Intermap for processing the polarimetric SAR data, and Victor Bulzgis for assisting with the figures.

Figure 1 Average Snow Pit Diagrams Showing Snow Structure

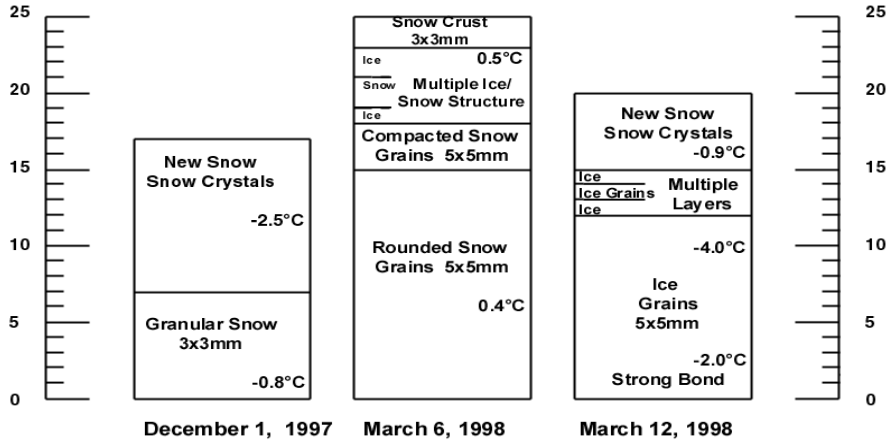

Figure 2 SWE Algorithm Values and Ground Measurements